Supplement of Atmos. Chem. Phys., 23, 9455–9471, 2023
https://doi.org/10.5194/acp-23-9455-2023-supplement

Atmospheric Chemistry and Physics
Open Access

Supplement of

High-time-resolution chemical composition and source apportionment of $PM_{2.5}$ in northern Chinese cities: implications for policy

Yong Zhang et al.

Correspondence to: Qiyuan Wang (wangqy@ieecas.cn) and Junji Cao (jjcao@mail.iap.ac.cn)

Text S1. Selcation of inputted HERM chemical species and its uncertainty calculation

Considering the validity and credibility of monitoring data, chemical species including OA, NO_3^-, SO_4^{2-}, NH_4^+, Cl^-, and BC were all selected to input HERM model for three pilot cities. For inorganic elements, Si, K, Ca, Cr, Mn, Fe, Ni, Cu, Zn, As, Se, Ba, and Pb in Xi'an and Beijing, and Si, K, Ca, Ti, Cr, Mn, Fe, Ni, Cu, Zn, As, Se, Ba, and Pb in Shijiazhuang were selected for source apportionment, respectively.

The uncertainty data of chemical species inputting HERM was calculated according to the recommendation in the PMF5.0 user guideline. If the measured chemical species concentration is greater than the minimum detection limit (MDL) provided, the uncertainty (Unc) calculation is based following equation:

$$Unc_i = \sqrt{(C_i \times E_i)^2 + (0.5 \times MDL_i)^2} \quad (1)$$

where C_i represents measured concertation for species i, E_i represents error fraction of species i. For online measured data, the error fraction was recommended to use 10% (Rai et al., 2020). If the measured concentration is less than or equal to the MDL provided, the Unc is calculated as the following equation:

$$Unc = \frac{5}{6} \times MDL \quad (2)$$

Text S2 Diagnostics of HERM solutions

In this study, factors numbering from two to ten were selected and run in the HERM software. Each factor solution was run thirty times with completely unconstrained profiles to explore the possible sources. The optimal factor number solution was determined by examining the ratio of Q and expected Q (Q_{exp}). The Q_{exp} in HERM was equal to (samples ×species – factors × (samples + species) + the number of constrained source profiles). As shown in Fig. S5, the value of Q/Q_{exp} decreased with the increase of the factor number, which suggests increasing the factor number could lead to a better explanation of the variance by HERM. However, the utility of increasing factors declined with the number of factors. Too many factors could cause splitting profiles, although the Q/Q_{exp} may be desirable (Liu et al., 2021; Salameh et al., 2018, 2016). Thus, the drops of Q/Q_{exp} ($\Delta Q/Q_{exp}$) were subsequently evaluated to choose the optimal solution factor number. As shown in Table S2, when the number of factors increases to more than six in Xi'an, the value of $\Delta Q/Q_{exp}$ shows a relatively stable change trend. A six-factor solution is preferable because $\Delta Q/Q_{exp}$ between the five-solution and six-solution is smaller than that between the six-solution and seven-solution (Liu et al., 2021). In addition, secondary formation source and biomass burning were mixed when the factor number was five, and vehicle emission was split into two profiles when the factor number was seven (Table

S3). Therefore, the six-factor solution was determined as the optimal HERM solution for Xi'an. Similar criterias were used for Shijiazhuang and Beijing, six-factor and eight-factor solutions were determined as optimal HERM solutions, respectively.

Text S3 Estimation of secondary organic aerosol (SOA).

Due to lack of critical tracers of SOA, the sources of SOA cannot be individually resolved by receptor model. In this study, In this study, the secondary sources were mainly characterized by high EV values for inorganic aerosols such as SO_4^{2-} , NO_3^-, NH_4^+, but the medium EV values for OA (16~29%) were also presented on secondary sources in three pilot cities. This means that the SOA maybe mixed in with the factors of secondary sources. To verify this, the SOA concentrations we estimated by using a BC-tracer method (Wang et al., 2019) and then compared the results with those based on source apportionment. The SOA calculation by BC-tracer method was calculated as follow:

$$[SOA]\_{BC\text{-}tracer} = [OA] - (OA/BC)_{pri} \times [BC] \quad (3)$$

where [ ] means mass concentration, $(OA/BC)_{pri}$ is the ratio of [OA] to [BC] in primary emission. The $(OA/BC)_{pri}$ ratios vary among sources, therefore, a minimum R squired (MRS) method was used to derive appropriate $(OA/BC)_{pri}$ values for three pilot cities. In previous studies (Srivastava et al., 2018; Wang et al., 2019), MRS method has been used to calculated the concertation of secondary organic carbon and brown carbon. More detailed information on the method and a validation of this approach can be found in Wang et al. (2019).

In addition, according to results of receptor model, SOA concentration can also be estimated as follow based on EV values of OA from secondary source factors.

$$[SOA]\_{source\ apportionment} = [OA] \times EV\_OA \quad (4)$$

where EV_OA represents the EV values of OA in secondary sources factors resolved by HERM model.

As shown in Fig. S9, the $(OA/BC)_{pri}$ ratios were determined as 4.73 for Xi'an, 3.12 for Shijiazhuang and 7.6 for Beijing, respectively. Furthermore, the concentrations of SOA from three pilot cities were shown in Table R1 based two different methods. As we can see, the SOA concentrations estimated by EV values of OA are close to that by BC-tracer method for three pilot cities. This indicated SOA was mixed in secondary sources factors.

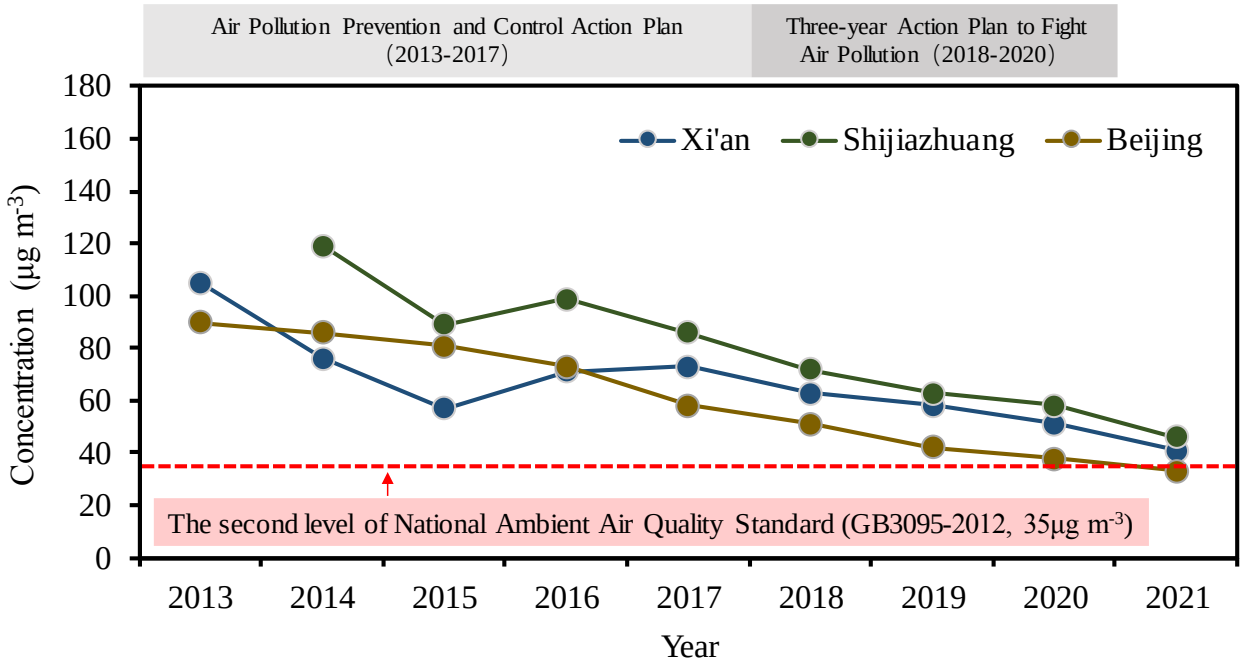

Figure S1. Annual average concentration of $PM_{2.5}$ from 2013 to 2021 in Xi'an, Shijiazhuang, and Beijing. (The data are from the website of the local Ecological Environment Bureau, Xi'an: http://xaepb.xa.gov.cn/, Shijiazhuang: https://sthjj.sjz.gov.cn/, Beijing: http://sthjj.beijing.gov.cn/). The red dotted line represents the second level of the National Ambient Air Quality Standard (GB3095-2012, 35 μg m^{-3})

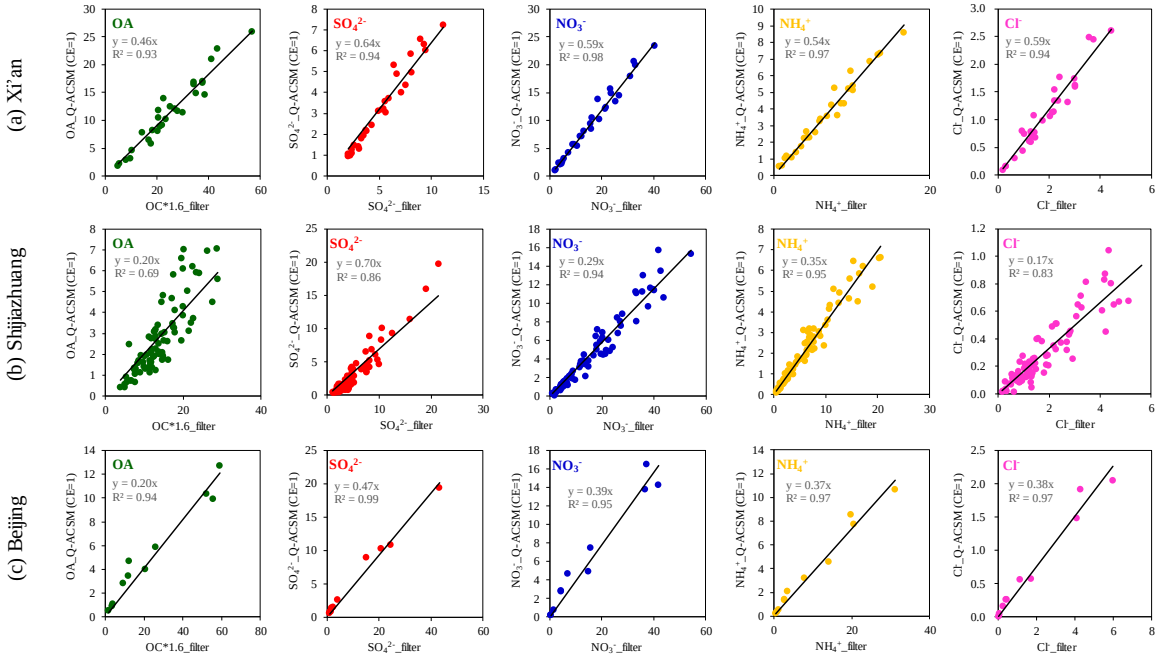

Figure S2. Correction of chemical components measured by Q-ACSM in different cities. During the campaigns, offline filter samples were simultaneously sampled for the correction. In summary, 29 offline samples in Xi'an, 83 offline samples in Shijiazhuang, and 10 offline samples in Beijing were sampled respectively.

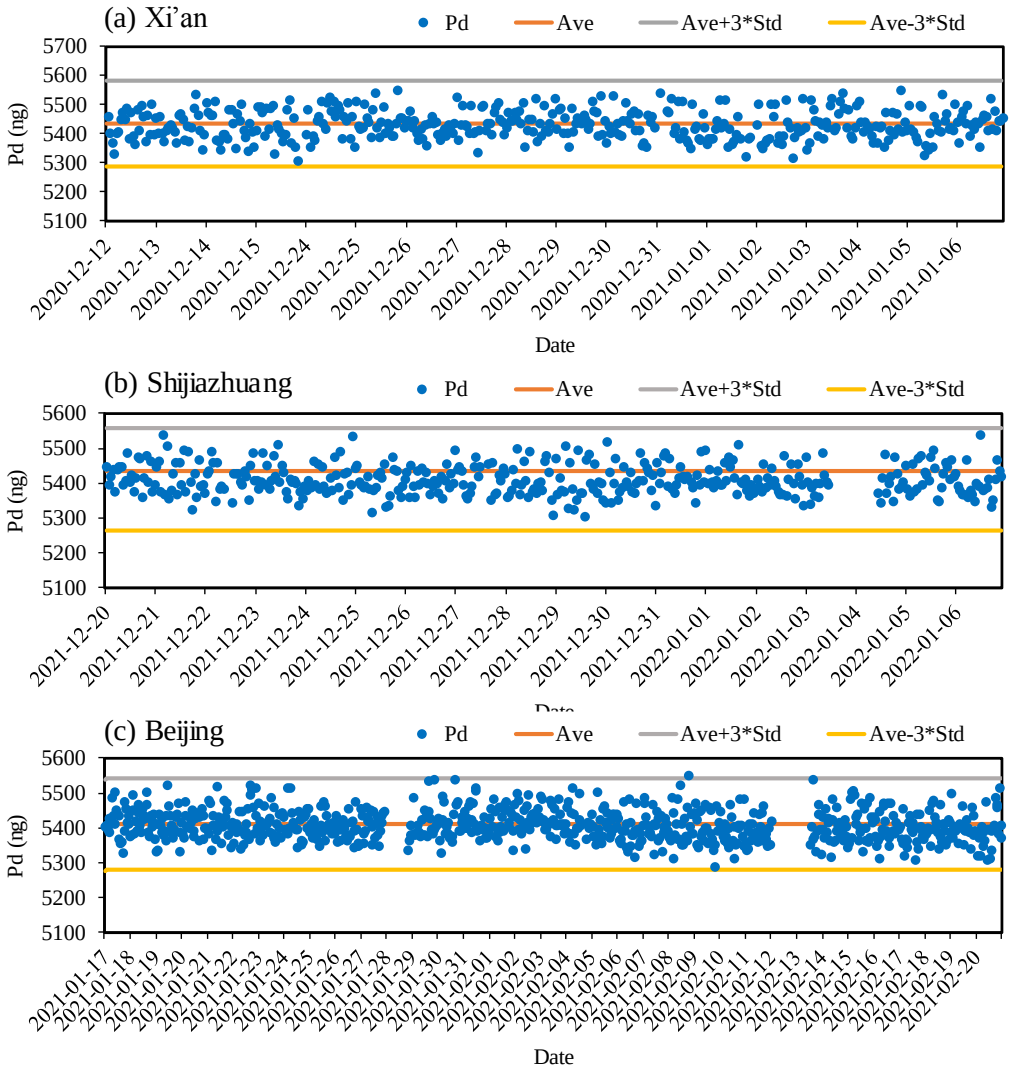

Figure S3. Concentration of the internal standard element (Pd) of Xact625 during sampling periods in (a) Xi'an, (b) Shijiazhuang, and (c) Beijing.

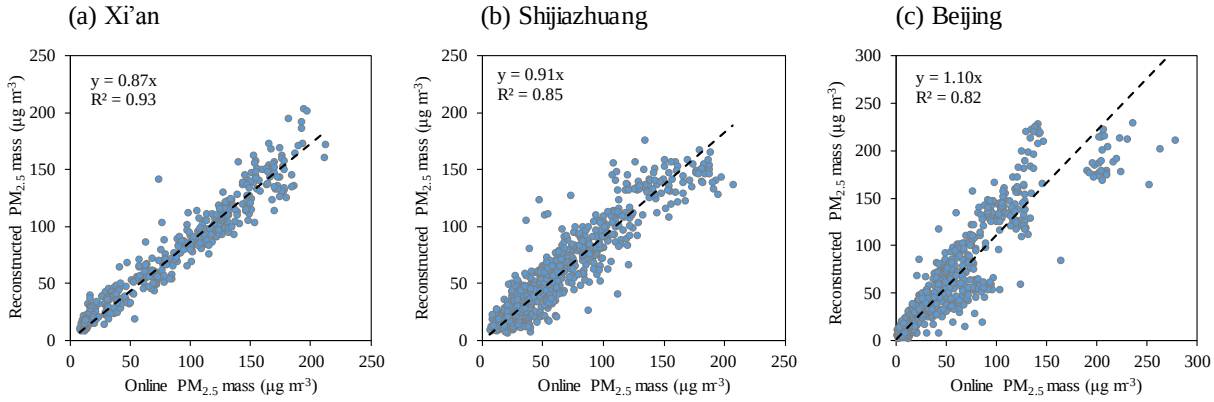

Figure S4. Correlation of online and reconstructed $PM_{2.5}$ concentration in (a) Xi'an, (b) Shijiazhuang, and (c) Beijing during the campaigns. The online $PM_{2.5}$ mass data in the X axis from national monitor stations near sampling sites.

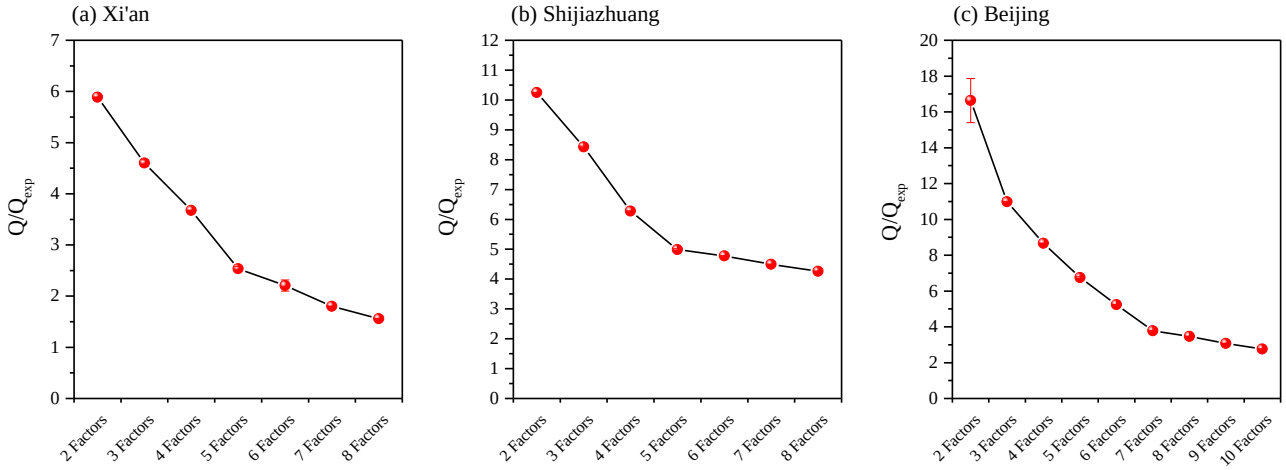

Figure S5. Values of Q/Q_{exp} for the unconstrained profile solutions with two to ten factors based on thirty runs in (a) Xi'an, (b) Shijiazhuang, and (c) Beijing, respectively.

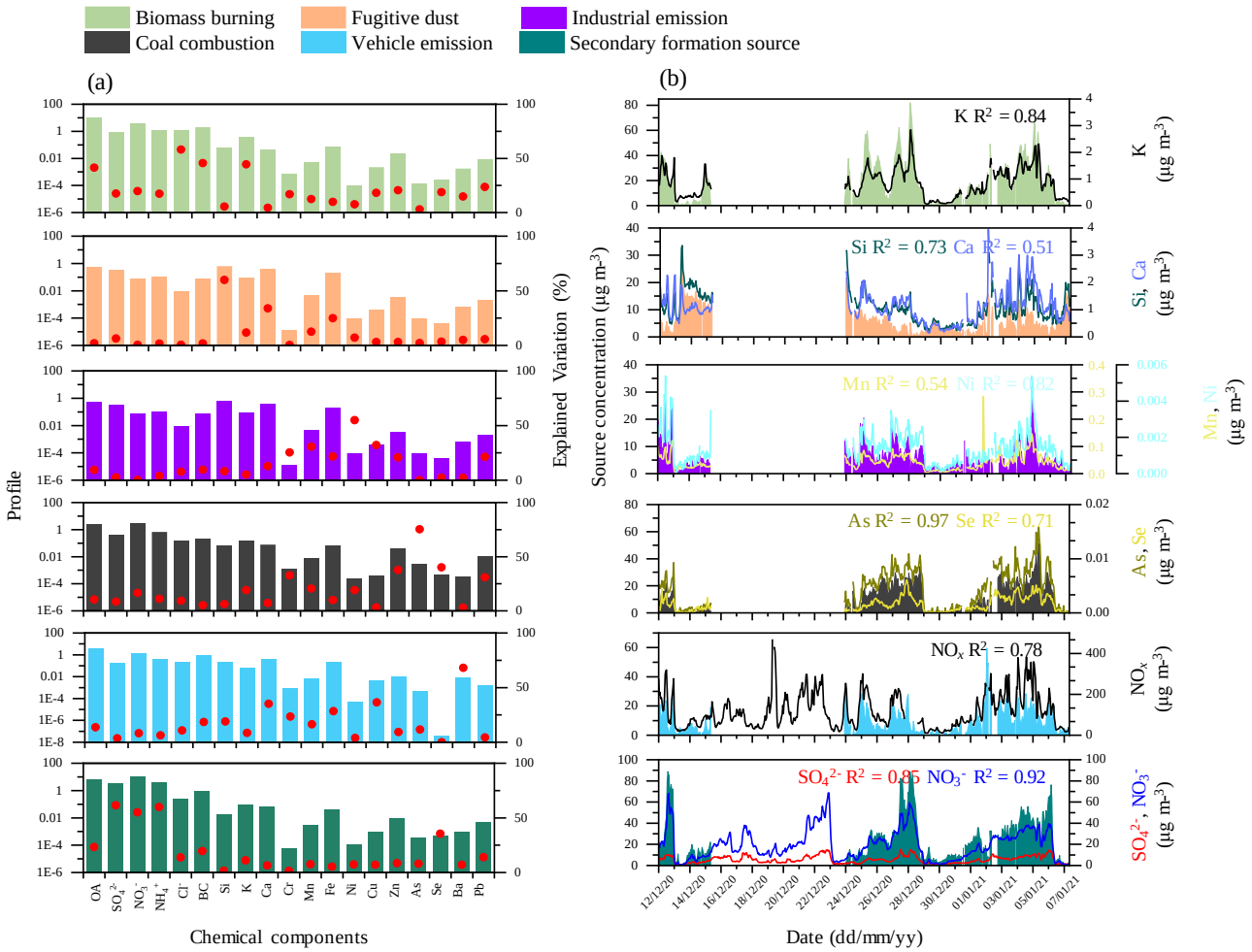

Figure S6. (a) Sources profiles obtained from HERM with a six-factor solution in Xi'an, the columns in each factor are the profile that displays the relative relation of the absolute values of variables. The red dot represents the explained variation (EV) in species for different factors. (b) Time series plots of sources concentration, including biomass burning, fugitive dust, industrial emission, coal combustion, vehicle emission, and secondary formation source. The corresponding time trends of chemical tracers are also shown.

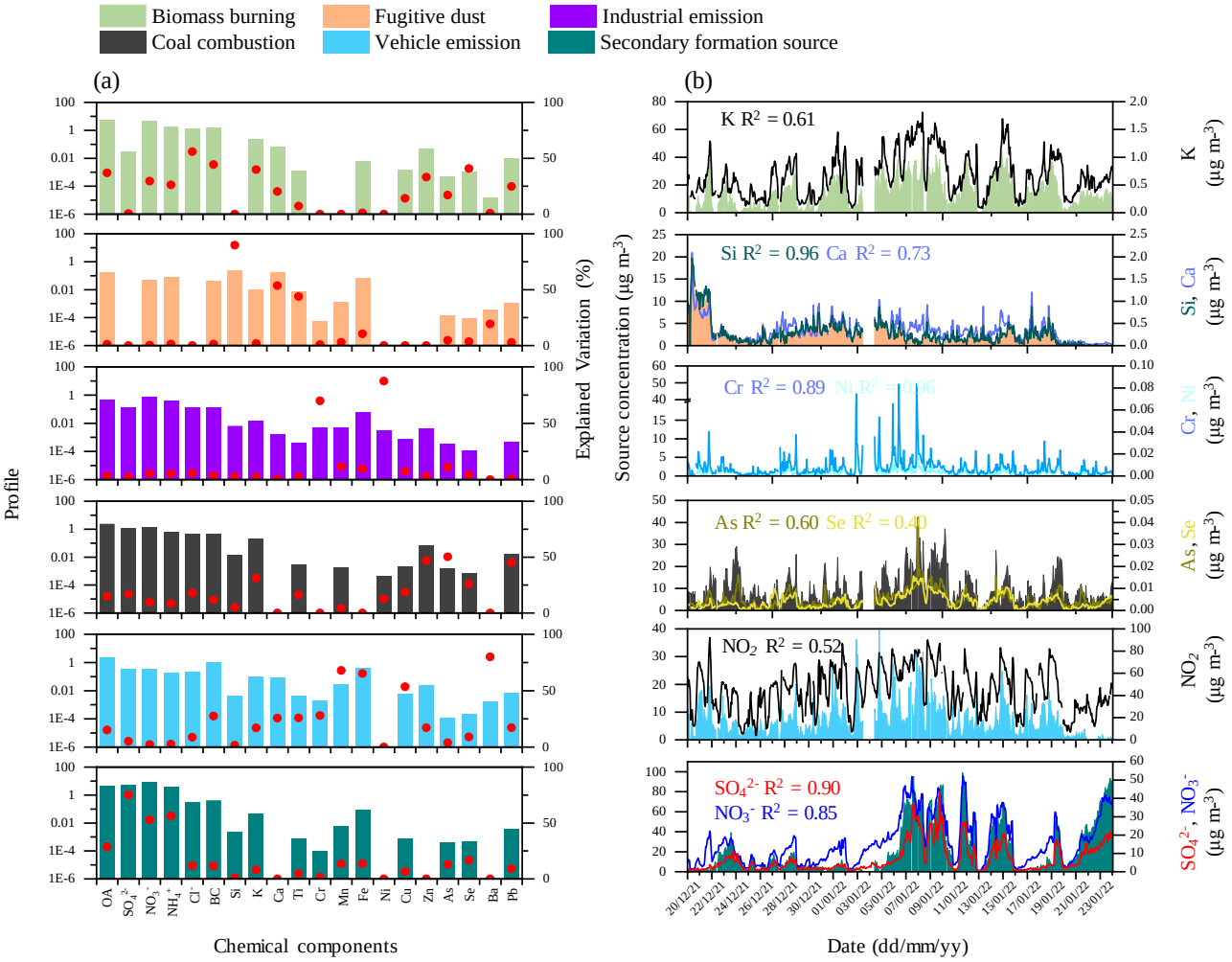

Figure S7. (a) Sources profiles obtained from HERM with a six-factor solution in Shijiazhuang, the columns in each factor are the profile that displays the relative relation of the absolute values of variables. The red dot represents the explained variation (EV) in species for different factors. (b) Time series plots of sources concentration, including biomass burning, fugitive dust, industrial emission, coal combustion, vehicle emission, and secondary formation source. The corresponding time trends of chemical tracers are also shown.

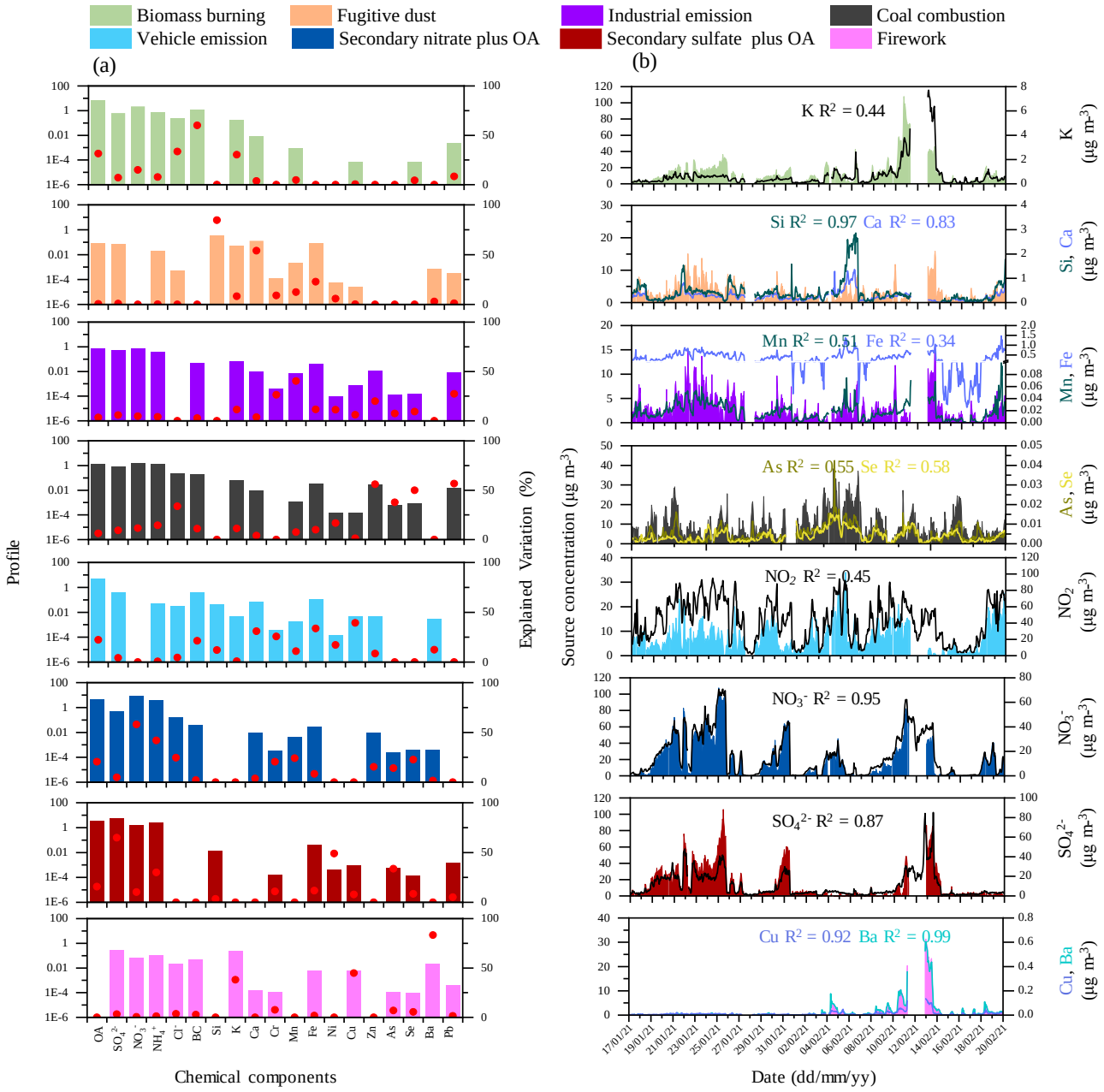

Figure S8. (a) Sources profiles obtained from HERM with an eight-factor solution in Beijing, the columns in each factor are the profile that displays the relative relation of the absolute values of variables. The red dot represents the explained variation (EV) in species for different factors. (b) Time series plots of sources concentration, including biomass burning, fugitive dust, industrial emission, coal combustion, vehicle emission, secondary nitrate plus OA, secondary sulfate plus OA, and firework. The corresponding time trends of chemical tracers are also shown.

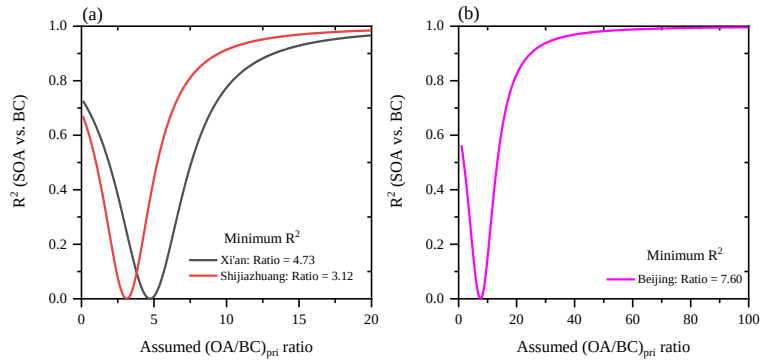

111

112 **Figure S9.** Coefficients of determination (R^2) for SOA versus BC mass concentration plotted against assumed

113 ratios for OA to BC in primary emissions ($(OA/BC)_{pri}$) in Xi'an, Shijiazhuang and Beijing.

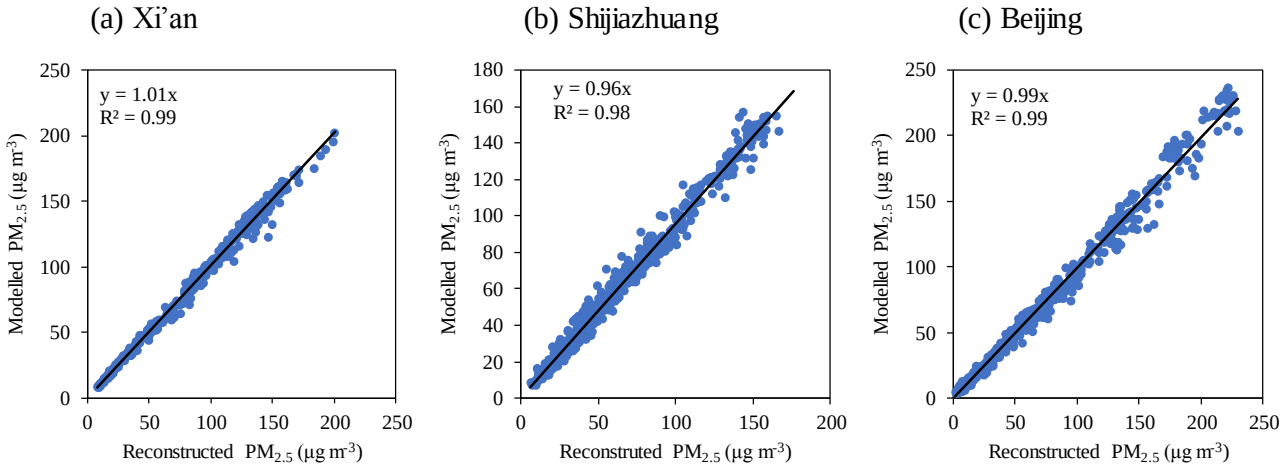

114

115 **Figure S10.** Correlation between reconstructed $PM_{2.5}$ and modeled $PM_{2.5}$ mass concentrations derived by HERM in

116 Xi'an, Shijiahuznag, and Beijing with optimal solutions

117

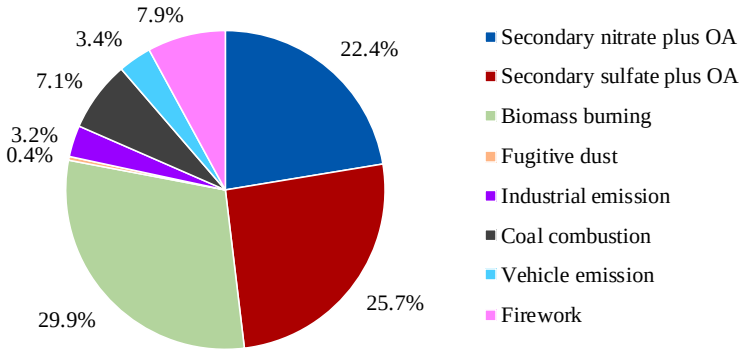

118

119 **Figure S11.** Source contribution of $PM_{2.5}$ during Chinese Spring Festival (from New Year's Eve to January 3rd of

120 the Lunar Calendar) in Beijing

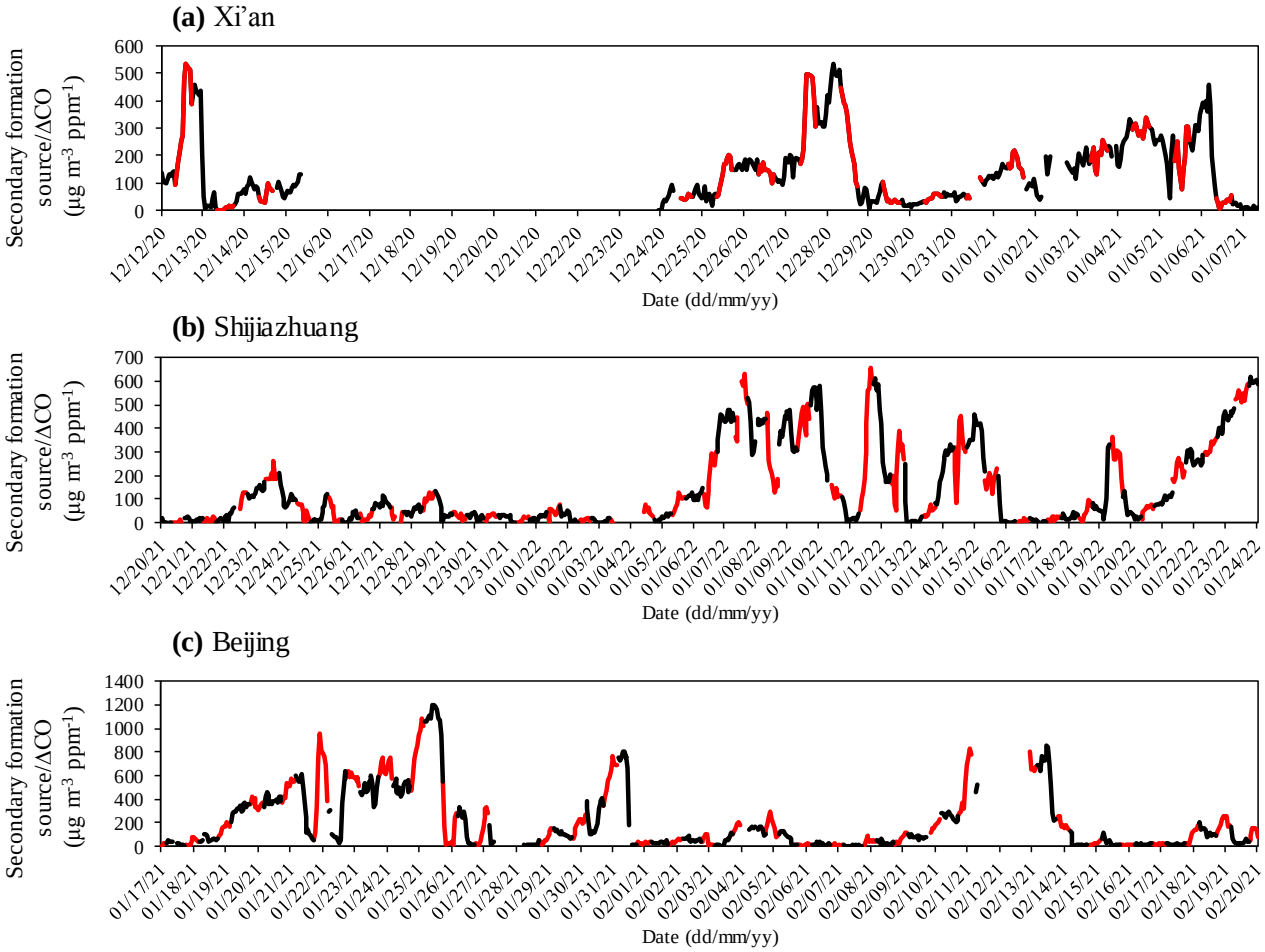

Figure S12. Time series plots of secondary formation source/ΔCO in (a) Xi'an, (b) Shijiazhuang, and (c) Beijing. The red and black lines represent daytime (08:00-17:00 LST) and nighttime (18:00 - 07:00 the next day LST), respectively.

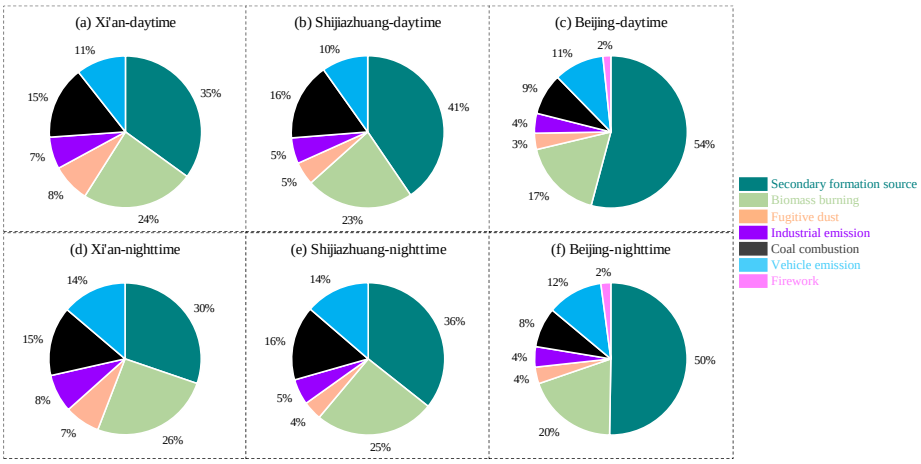

126

127 **Figure S13.** Source contribution of $PM_{2.5}$ in three pilot cities during daytime and nighttime, respectively.

128

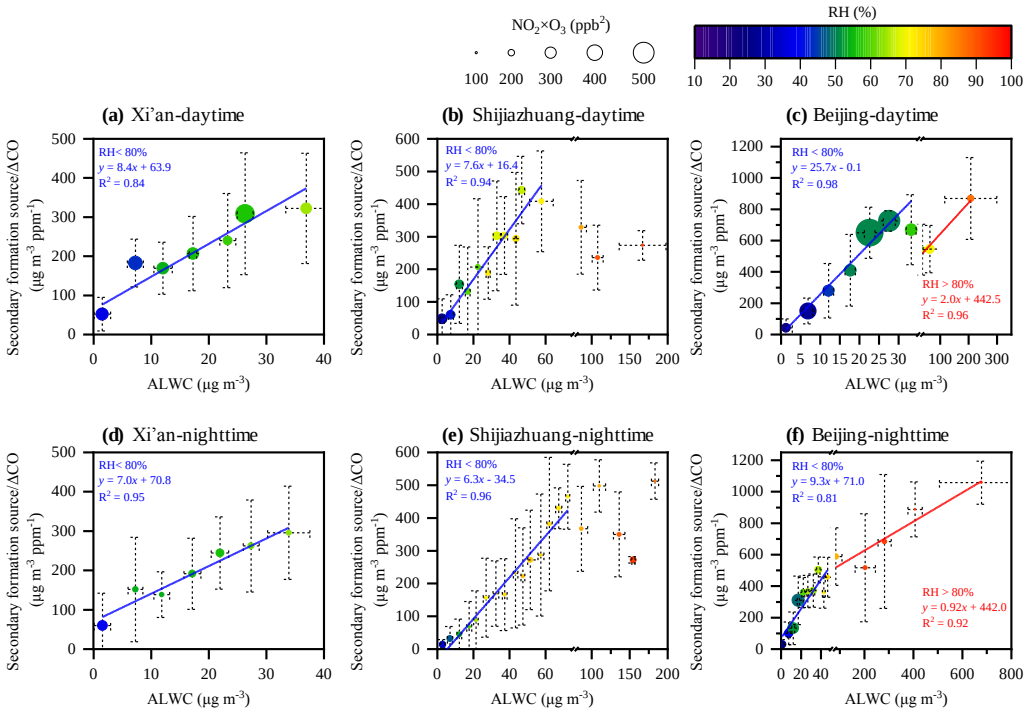

129

130 **Figure S14.** Correlation of secondary formation source/ΔCO and ALWC during daytime (08:00–17:00 LST, a–c)
131 and nighttime (18:00–7:00 the next day LST, d–f) in Xi'an, Shijiazhuang, and Beijing, respectively. The points and
132 error bar represent the mean values and standard deviation values of secondary formation source /ΔCO and ALWC
133 in each bin. In Xi'an, each bin is 5 μg m^{-3} (ΔALWC = 5 μg m^{-3}). In Shijiazhuang, each bin is 5 μg m^{-3} (ΔALWC = 5
134 μg m^{-3}) when ALWC ranged from 0 to 75μg m^{-3}, but 25 μg m^{-3} (ΔALWC = 25 μg m^{-3}) for ALWC ranged from 75 to
135 200 μg m^{-3} due to limitations in data. In Beijing, during daytime, each bin is 5 μg m^{-3} (ΔALWC = 5 μg m^{-3}) when
136 ALWC ranged from 0 to 40 μg m^{-3}, but 100 μg m^{-3} (ΔALWC = 100 μg m^{-3}) for ALWC ranged from 40 to 450 μg m^{-3} due to limitations in data. During nighttime, each bin is 5 μg m^{-3} (ΔALWC = 5 μg m^{-3}) when ALWC ranged from 0
137 to 50 μg m^{-3}, but 100 μg m^{-3} (ΔALWC = 100 μg m^{-3}) for ALWC ranged from 50 to 900 μg m^{-3} due to limitations in
138 data.
139

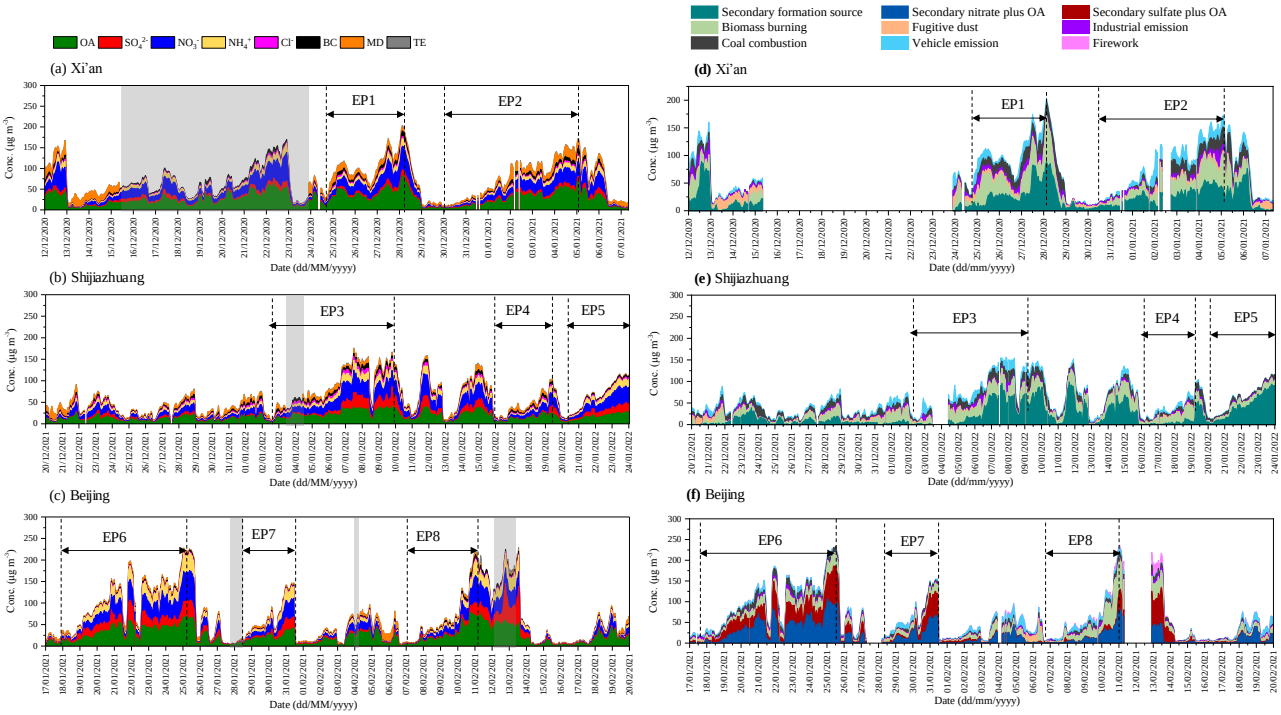

Figure S15. The pollution episodes selection according to temporal variation of $PM_{2.5}$ chemical components (a-c) and source contribution (d-f) during the campaigns in Xi'an, Shijiazhuang, and Beijing, respectively. The gray shape parts were lack of MD values due to the out-of-order Xact625, and missing values in the time series owing to the out-of-order ACSM, AE33, and Xact625 at the same time.

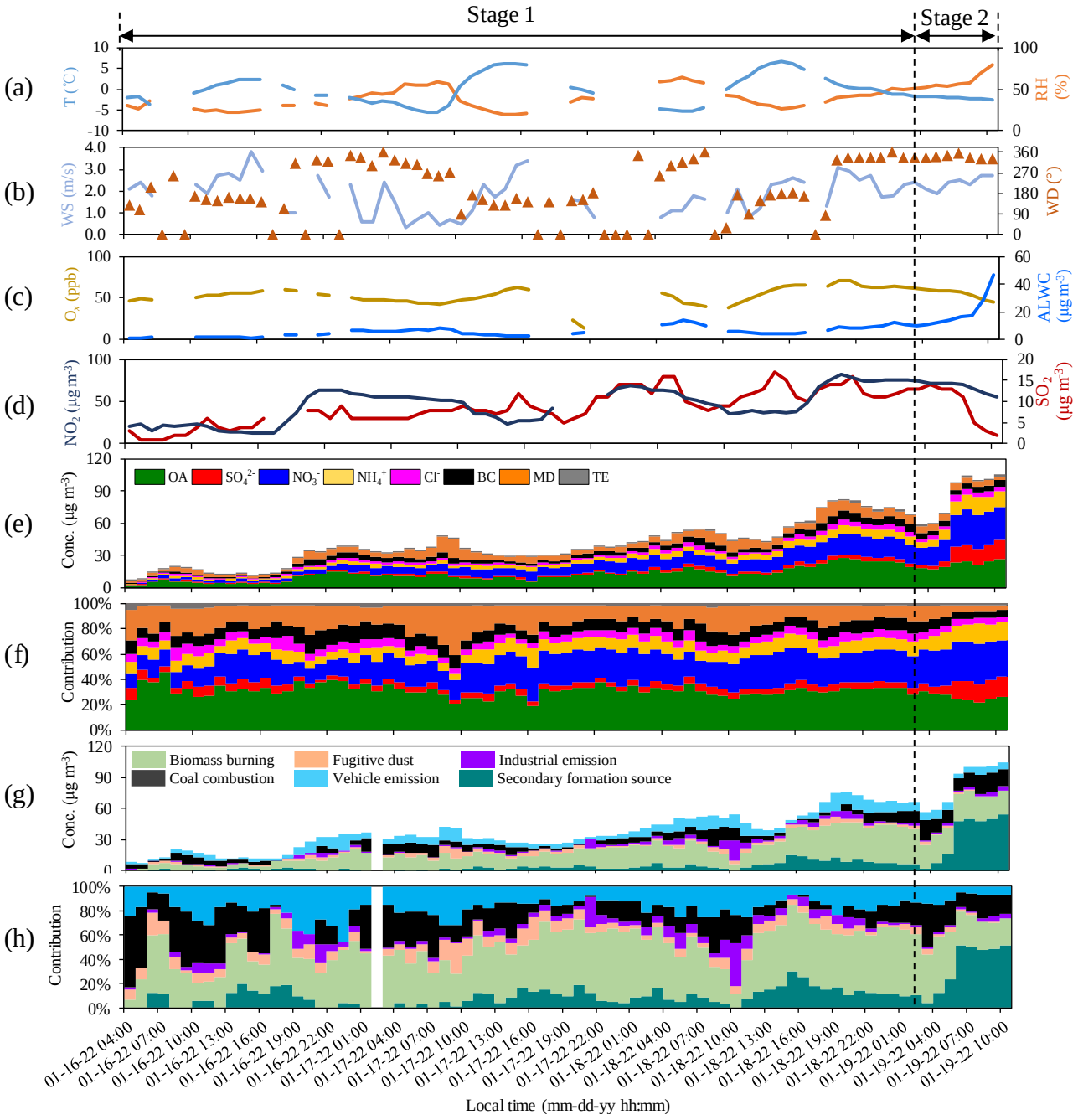

Figure S16. Time series of T and RH (a), WS and WD (b), O_x and ALWC (c), NO_2 and SO_2 (d), chemical components (e,f), and source contribution (g, h) of $PM_{2.5}$ during EP4 in Shijiazhuang.

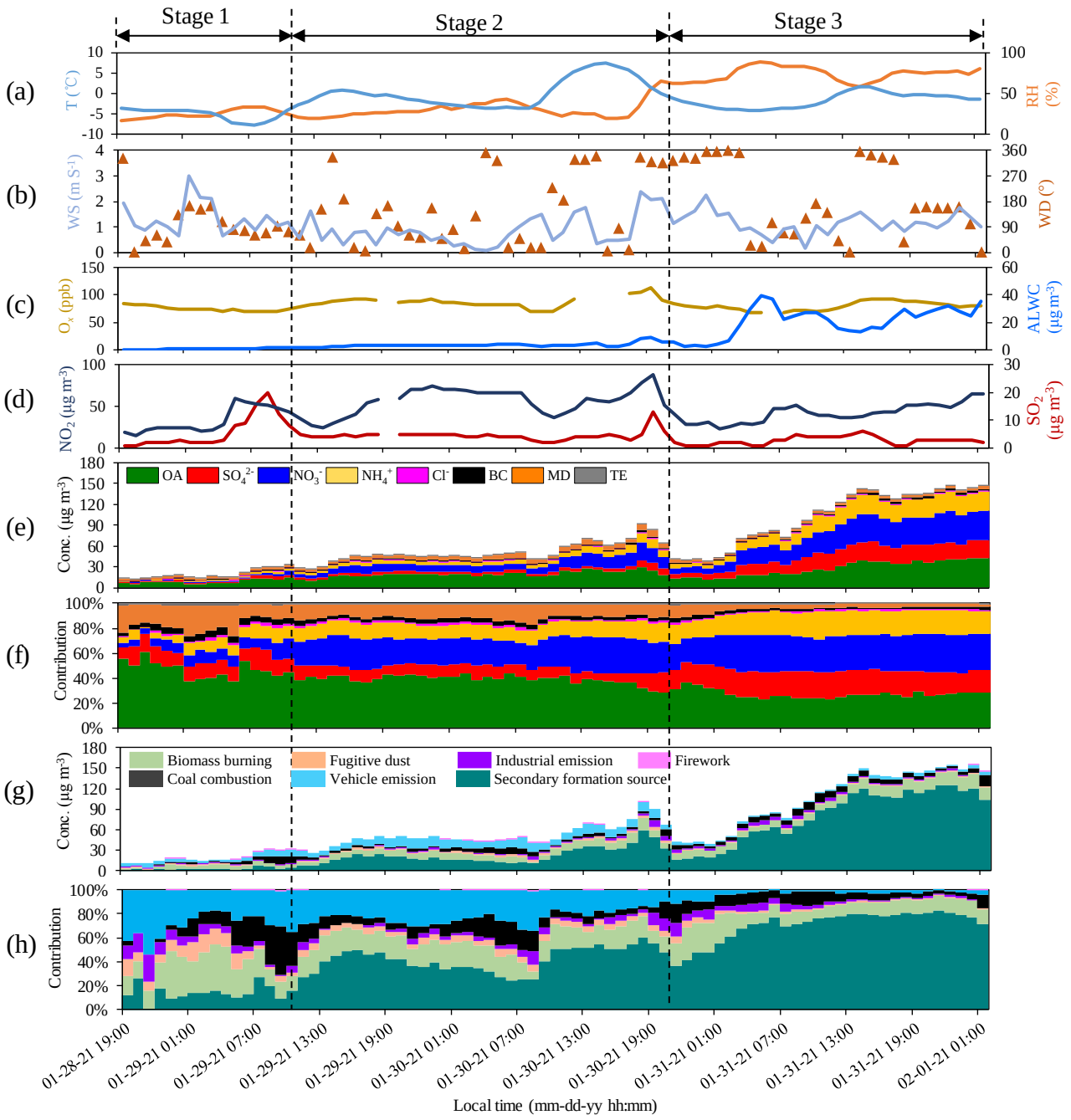

Figure S17. Time series of T and RH (a), WS and WD (b), O_x and ALWC (c), NO_2 and SO_2 (d), chemical components (e, f), and source contribution (g, h) of $PM_{2.5}$ during EP7 in Beijing

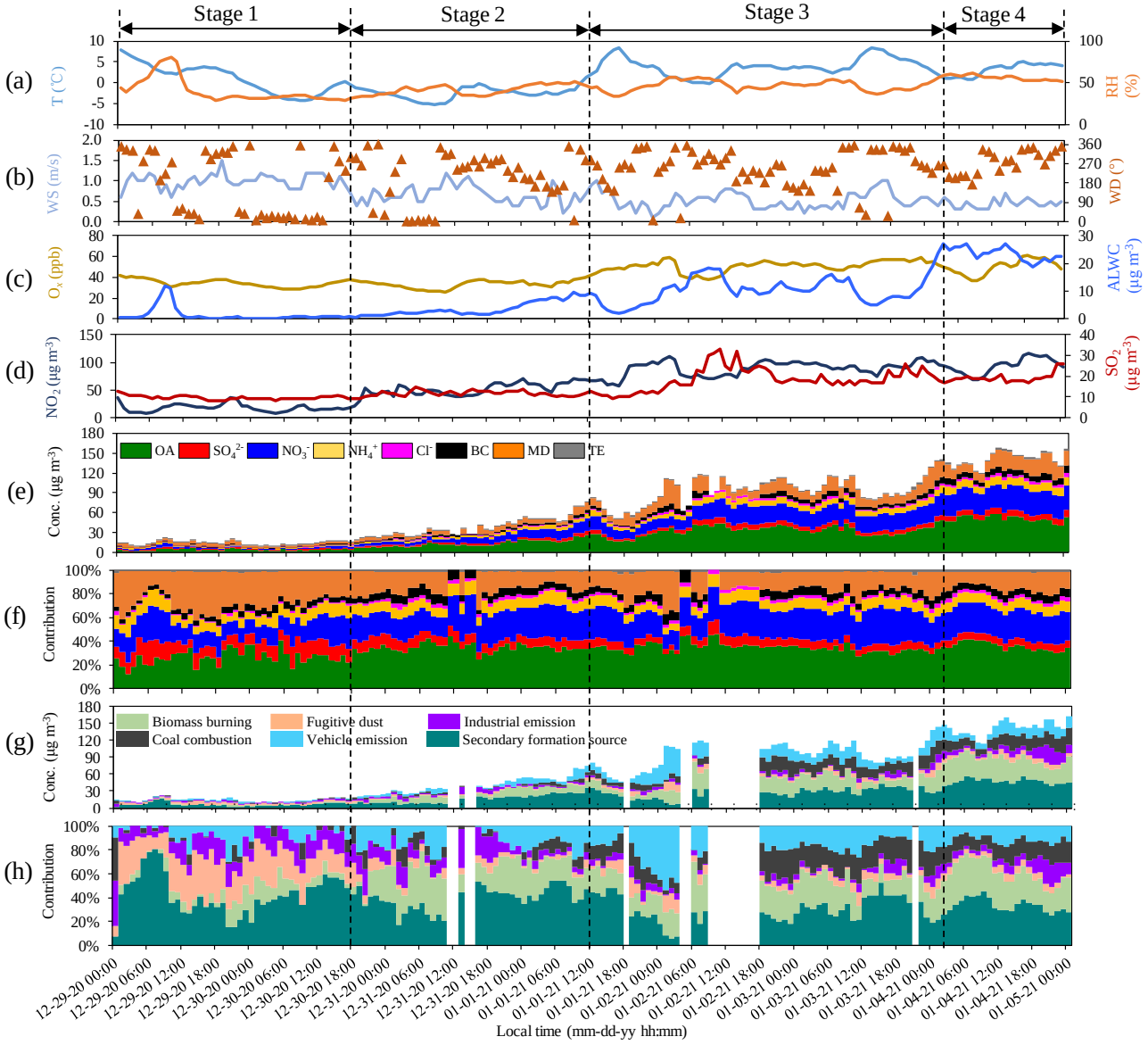

Figure S18. Time series of T and RH (a), WS and WD (b), O_x and ALWC (c), NO_2 and SO_2 (d), chemical components (e, f), and source contribution (g, h) of $PM_{2.5}$ during EP2 in Xi'an.

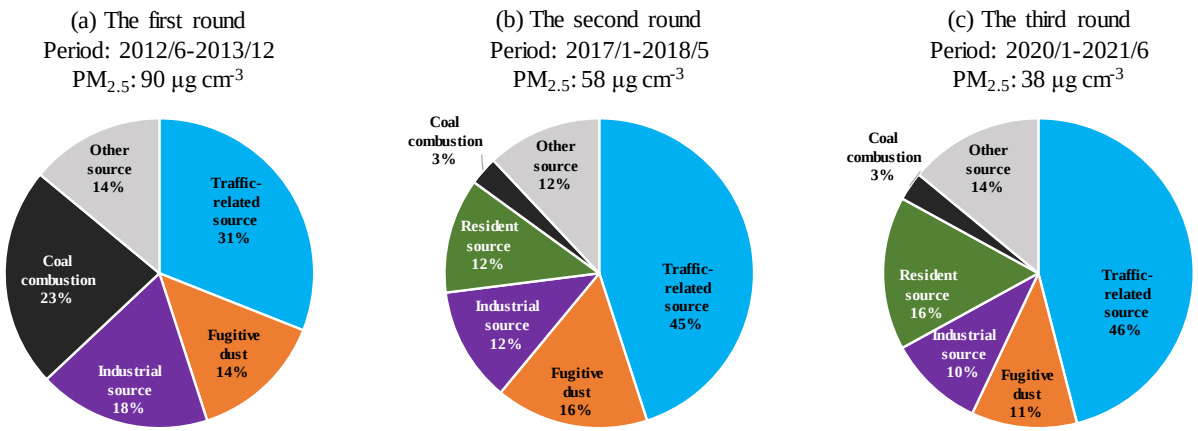

159

160 **Figure S19.** $PM_{2.5}$ sources apportionment in Beijing released by Beijing Municipal Ecology and Environment
161 Bureau in the last decade (http://sthjj.beijing.gov.cn/so/s?tab=all&sourceCode=1100000122, in Chinese).
162

Table S1. Detailed information on complementary data for sampling sites

Sampling site	National Air Quality Monitoring Station	National Meteorological Station	complementary data
Xi'an	Gaoxinxiqu station, 1.1km from the sampling site	Haidian station, 7.6 km from the sampling site	hourly $PM_{2.5}$, NO_x, NO_2, CO, SO_2, O_3, WS, WD, T, RH
Shijiazhuang	Gaoxinqu station, 4.2 km from the sampling site	Shijiazhuang station, 23.8 km from the sampling site	hourly $PM_{2.5}$, NO_2, CO, SO_2, O_3, WS, WD, T, RH
Beijing	ChaoyangAotizhongxin station, 1.2 km from the sampling site	Jinghe station, 21.2 km from the sampling site	hourly $PM_{2.5}$, NO_2, CO, SO_2, O_3, WS, WD, T, RH

Note: WS: wind speed, WD: wind direction, T: temperature, RH: relative humidity.

Table S2. The $\Delta Q/Q_{exp}$[a] value with increasing factor number from two to ten of the runs in Xi'an, Shijiazhuang, and Beijing.

Parameter[b]	$\Delta Q/Q_{exp}$		
	Xi'an	Shijiazhuang	Beijing
F2-F3	1.3	1.8	5.7
F3-F4	0.9	2.2	2.3
F4-F5	1.1	1.2	1.9
F5-F6	0.4	0.3	1.5
F6-F7	0.3	0.3	1.5
F7-F8	0.2	0.2	0.3
F8-F9			0.4
F9-F10			0.3

[a] $\Delta Q/Q_{exp}$ means the difference of Q/Q_{exp} of two sequent factor numbers.

[b] Parameters represent the factor numbers (F) – (F+1).

Table S3. Sources diagnostics with increasing factor numbers from four to ten of the runs in Xi'an, Shijiazhuang, and Beijing.

Factor number	Sources identification		
	Xi'an	**Shijiazhuang**	**Beijing**
4	Secondary formation source mixed with biomass burning and coal burning mixed with industrial emission	i) Secondary formation source mixed with primary sources including biomass burning and coal combustion ii) Biomass burning, coal combustion, and vehicle emission was also mixed	i) Secondary sources mixed with primary sources including biomass burning, coal combustion, and vehicle emission ii) Biomass burning and coal combustion was mixed
5	Secondary formation source mixed with biomass burning	Biomass burning, coal combustion, and vehicle emissions were mixed	Secondary sulfate plus OA mixed with coal combustion and industrial emission; secondary nitrate plus OA mixed with biomass burning
6	Six individual sources were identified	Six individual sources were identified	Secondary sulfate plus OA mixed with coal combustion and secondary nitrate plus OA mixed with industrial emission
7	Vehicle emission was split into two profiles	Coal combustion was split into two profiles	Secondary sulfate plus OA mixed with coal combustion
8	Vehicle emission and industrial emission was split into two profiles, respectively.	Vehicle emission and coal combustion were split into two profiles, respectively.	Eight individual sources were identified
9			Coal combustion was split into two profiles
10			Coal combustion and biomass burning were split into two profiles, respectively.

Table S4. Average concentrations of reconstructed $PM_{2.5}$ and its chemical species in Xi'an, Shijiazhuang, and Beijing during the campaign* (μg m^{-3})

Chemical Species	Xi'an	Shijiazhuang	Beijing
Reconstructed $PM_{2.5}$	77 ± 47	60 ± 39	64 ± 57
OA	25.9 ± 18.0	16.0 ± 9.7	22.1 ± 18.1
SO_4^{2-}	5.2 ± 3.4	7.0 ± 7.6	9.6 ± 11.3
NO_3^-	18.5 ± 14.5	15.8 ± 12.5	15.2 ± 16.7
NH_4^+	6.2 ± 4.5	7.0 ± 5.5	9.2 ± 10.3
Cl^-	1.9 ± 1.5	2.8 ± 2.2	0.7 ± 0.8
BC	4.5 ± 3.2	3.9 ± 2.5	1.9 ± 1.8
MD[a]	13.2 ± 7.0	6.0 ± 4.0	4.8 ± 3.8
TE[b]	1.1 ± 0.7	1.0 ± 0.6	0.9 ± 1.5

* Data during Xact625 failure shown in Figure S2 was excluded to calculate average concentration of campaign

[a] MD means mineral dust, which is equal to 2.20Al + 2.49Si + 1.63Ca + 2.42Fe + 1.94Ti

[b] TE means trace elements which is equal to K + Cr + Mn + Ni + Cu + Zn + As +Se + Ba + Pb

Table S5. The nitrogen oxidation ratio (NOR) and sulfur oxidation ratio (SOR) in Xi'an, Beijing, and Shijiazhuang during the campaigns[a]

Parameters	Xi'an	Shijiazhuang	Beijing
NOR	0.15 ± 0.08	0.20 ± 0.11	0.16 ± 0.12
SOR	0.18 ± 0.08	0.36 ± 0.25	0.48 ± 0.23

[a] $NOR = n(NO_3^-)/(n(NO_3^-) + n(NO_2))$; $SOR = n(SO_4^{2-})/(n(SO_4^{2-}) + n(SO_2))$. where $n(NO_3^-)$, $n(NO_2)$, $n(SO_4^{2-})$, and $n(SO_2)$ are the molar concentrations of NO_3^-, NO_2, SO_4^{2-}, and SO_2, respectively.

Table S6. Average concentrations of SOA in Xi'an, Shijiazhuang, and Beijing during sampling periods estimated by BC-tracer method and source apportionment results (μg m^{-3})

SOA	Xi'an	Shijiazhuang	Beijing
$SOA_{\_BC\text{-}tracer}$	5.1 ± 5.8	4.2 ± 4.4	8.0 ± 9.0
$SOA_{\_source\ apportionment}$	6.0 ± 4.1	4.6 ± 2.8	8.2 ± 6.7

Table S7. The concentration of $PM_{2.5}$ and its main chemical components during wintertime in Xi'an, Shijiazhuang, and Beijing in the last decades.

City	Year	$PM_{2.5}$	OA[a]	EC	SO_4^{2-}	NO_3^-	NH_4^+	Others	References
		μg m^{-3}	μg m^{-3}	μg m^{-3}	μg m^{-3}	μg m^{-3}	μg m^{-3}	μg m^{-3}	
Xi'an	2003	356	153.3	21.5	53.8	29.2	29.6	68.9	Cao et al., 2012
	2006	230	57.4	11.4	45.9	20.6	14.2	80.0	Xu et al., 2016
	2008	199	48.3	9.9	42.5	20.8	11.0	66.9	Xu et al., 2016
	2010	233	60.0	14.7	30.6	22.9	12.3	92.8	Xu et al., 2016
	2012	196	56.3	8.2	27.0	19.2	13.3	71.9	Zhang et al., 2015
	2013	263	45.8	7.1	31.7	29.2	17.1	132.5	Niu et al., 2016
	2014	156	57.4	2.5	16.2	20.6	9.4	49.7	Dai et al., 2018
	2018	189	42.1	4.9	9.7	14.5	6.6	111.0	Wang et al., 2022
	2020*	77	25.9	4.5	5.2	18.5	6.2	16.2	This study
Shijiazhuang	2010	227	75.6	12.2	33.2	25.3	10.5	70.2	Zhao et al., 2013
	2015	232	82.0	16.3	26.6	27.4	19.8	59.7	Huang et al., 2017
	2016	193	63.2	13.5	29.5	24.0	17.0	45.8	Liu et al., 2019
	2017	97	31.2	6.5	12.5	16.5	12.5	17.8	Liu et al., 2019
	2018	96	35.8	10.1	10.5	15.3	6.3	18.0	Zhang et al., 2020
	2022*	60	16.0	3.9	7.0	15.8	7.0	9.8	This study
Beijing	2001	122	51.5	11.3	9.9	10.7	7.1	31.5	Duan et al., 2006
	2003	116	38.2	6.2	20.0	13.1	9.4	29.1	Cao et al., 2012
	2004	107	53.8	8.3	12.7	8.3	6.0	17.9	Song et al., 2007
	2010	127	42.9	7.1	14.2	17.1	5.2	40.5	Zhao et al., 2013
	2013	132	38.5	6.4	21.9	18.5	15.1	31.6	Tao et al., 2015
	2014	138	46.4	5.2	21.0	26.0	14.1	25.3	Ma et al., 2017
	2016	130	75.7	20.2	12.3	5.5	10.5	5.3	Xu et al., 2018
	2021*	64	22.1	1.9	9.6	15.2	9.2	6.4	This study

* study was conducted on online monitoring equipment, and the rest studies were researched on filter sampling experiments.

[a] Assumption of OA = 1.6 × OC for the filter-based sampling experiments

Table S8. The concentration of $PM_{2.5}$ and its source contribution during wintertime in Xi'an, Shijiazhuang, and Beijing in the last decades.

City	Year	$PM_{2.5}$	Vehicle emission	Coal combustion	Secondary formation source	Fugitive dust	Industrial emission	Biomass burning	Others	References
		μg m^{-3}	μg m^{-3}	μg m^{-3}	μg m^{-3}	μg m^{-3}	μg m^{-3}	μg m^{-3}	μg m^{-3}	
Xi'an	2006	392	74.5	121.5	82.3	51.0	39.2	23.5		Xu et al., 2016
	2008	199	41.8	55.7	45.8	23.9	21.9	10.0		Xu et al., 2016
	2010	233	48.9	55.9	41.9	44.3	30.3	11.7		Xu et al., 2016
	2014	169	20.3	47.3	71.0	8.5	6.8	15.2		Dai et al., 2020
	2018	189	26.5	28.4		15.1	22.7	58.6	37.8	Wang et al., 2022
	2020*	77	10.0	11.6	24.6	6.2	6.2	19.3		This study
Shijiazhuang	2015	232	46.4	62.6	30.2	20.9	16.2	7.0	48.7	Huang et al., 2017
	2016	181	23.5	54.3	54.3	30.8	9.1		7.2	Liu et al., 2018
	2019	119	21.4	21.4	42.8	21.4	6.0	6.0		Diao et al., 2021
	2022*	60	7.2	9.6	22.8	2.4	3.0	14.4		This study
Beijing	2004	107	8.6	40.7	19.3	7.5		16.1	15.0	Song et al., 2007
	2010	139		79.2	8.3	22.2	16.7	9.7	2.8	Zhang et al., 2013
	2013	159	9.5	41.3	79.5	15.9		9.5	3.2	Huang et al., 2014
	2015	125	48.8	15.0	23.8	8.8	2.5	6.3	18.8	Huang et al., 2017
	2021*	64	7.0	5.8	33.3	2.6	2.6	11.5	1.3	This study

* study was conducted on online monitoring equipment, and the rest studies were researched on filter sampling experiments.

References:

Cao, J.-J., Shen, Z.-X., Chow, J. C., Watson, J. G., Lee, S.-C., Tie, X.-X., Ho, K.-F., Wang, G.-H., and Han, Y.-M.: Winter and summer $PM_{2.5}$ chemical compositions in fourteen Chinese cities, J. Air Waste Manage., 62, 1214–1226, https://doi.org/10.1080/10962247.2012.701193, 2012.

Chen, L., Lowenthal, D., Watson, J., Koracin, D., Kumar, N., Knipping, E., Wheeler, N., Craig, K., Reid, S.: Toward effective source apportionment using positive matrix factorization: experiments with simulated $PM_{2.5}$ data. J. Air Waste Manage., 60(1), 43–54, https://doi.org/10.3155/1047-3289.60.1.43, 2010.

Dai, Q., Bi, X., Liu, B., Li, L., Ding, J., Song, W., Bi, S., Schulze, B. C., Song, C., Wu, J., Zhang, Y., Feng, Y., and Hopke, P. K.: Chemical nature of $PM_{2.5}$ and PM_{10} in Xi'an, China: Insights into primary emissions and secondary particle formation, Environ. Pollut., 240, 155–166, https://doi.org/10.1016/j.envpol.2018.04.111, 2018.

Dai, Q., Hopke, P. K., Bi, X., and Feng, Y.: Improving apportionment of $PM_{2.5}$ using multisite PMF by constraining G-values with a prioriinformation, Sci. Total Environ., 736, 139657, https://doi.org/10.1016/j.scitotenv.2020.139657, 2020.

Diao, L., Zhang, H., Liu, B., Dai, C., Zhang, Y., Dai, Q., Bi, X., Zhang, L., Song, C., and Feng, Y.: Health risks of inhaled selected toxic elements during the haze episodes in Shijiazhuang, China: Insight into critical risk sources, Environ. Pollut., 276, 116664, https://doi.org/10.1016/j.envpol.2021.116664, 2021.

Duan, F., He, K., Ma, Y., Yang, F., Yu, X., Cadle, S., Chan, T., and Mulawa, P.: Concentration and chemical characteristics of $PM_{2.5}$ in Beijing, China: 2001–2002, Sci. Total Environ., 355, 264–275, https://doi.org/10.1016/j.scitotenv.2005.03.001, 2006.

Huang, R.-J., Zhang, Y., Bozzetti, C., Ho, K.-F., Cao, J.-J., Han, Y., Daellenbach, K. R., Slowik, J. G., Platt, S. M., Canonaco, F., Zotter, P., Wolf, R., Pieber, S. M., Bruns, E. A., Crippa, M., Ciarelli, G., Piazzalunga, A., Schwikowski, M., Abbaszade, G., Schnelle-Kreis, J., Zimmermann, R., An, Z., Szidat, S., Baltensperger, U., Haddad, I. E., and Prévôt, A. S. H.: High secondary aerosol contribution to particulate pollution during haze events in China, Nature, 514, 218–222, https://doi.org/10.1038/nature13774, 2014.

Huang, X., Liu, Z., Liu, J., Hu, B., Wen, T., Tang, G., Zhang, J., Wu, F., Ji, D., Wang, L., and Wang, Y.: Chemical characterization and source identification of $PM_{2.5}$ at multiple sites in the Beijing–Tianjin–Hebei region, China, Atmos. Chem. Phys., 17, 12941–12962, https://doi.org/10.5194/acp-17-12941-2017, 2017.

Liu, B., Cheng, Y., Zhou, M., Liang, D., Dai, Q., Wang, L., Jin, W., Zhang, L., Ren, Y., Zhou, J., Dai, C., Xu, J., Wang, J., Feng, Y., and Zhang, Y.: Effectiveness evaluation of temporary emission control action in 2016 in winter in Shijiazhuang, China, Atmos. Chem. Phys., 18, 7019–7039, https://doi.org/10.5194/acp-18-7019-2018, 2018.

Liu, G., Xin, J., Wang, X., Si, R., Ma, Y., Wen, T., Zhao, L., Zhao, D., Wang, Y., and Gao, W.: Impact of the coal banning zone on visibility in the Beijing-Tianjin-Hebei region, Sci. Total Environ., 692, 402–410, https://doi.org/10.1016/j.scitotenv.2019.07.006, 2019.

Liu, H., Wang, Q., Ye, J., Su, X. li, Zhang, T., Zhang, Y., Tian, J., Dong, Y., Chen, Y., Zhu, C., Han, Y., and Cao, J.: Changes in Source - Specific Black Carbon Aerosol and the Induced Radiative Effects Due to the COVID - 19 Lockdown, Geophys. Res. Lett., 48, https://doi.org/10.1029/2021GL092987, 2021.

Ma, Q., Wu, Y., Tao, J., Xia, Y., Liu, X., Zhang, D., Han, Z., Zhang, X., and Zhang, R.: Variations of Chemical Composition and Source Apportionment of $PM_{2.5}$ during Winter Haze Episodes in Beijing, Aerosol Air Qual. Res., 17, 2791–2803, https://doi.org/10.4209/aaqr.2017.10.0366, 2017.

Niu, X., Cao, J., Shen, Z., Ho, S. S. H., Tie, X., Zhao, S., Xu, H., Zhang, T., and Huang, R.: $PM_{2.5}$ from the Guanzhong Plain: Chemical composition and implications for emission reductions, Atmos. Environ., 147, 458–469, https://doi.org/10.1016/j.atmosenv.2016.10.029, 2016.

Rai, P., Furger, M., Slowik, J. G., Canonaco, F., Fröhlich, R., Hüglin, C., Minguillón, M. C., Petterson, K., Baltensperger, U., and Prévôt, A. S. H.: Source apportionment of highly time-resolved elements during a firework episode from a rural freeway site in Switzerland, Atmos. Chem. Phys., 20, 1657–1674, https://doi.org/10.5194/acp-20-1657-2020, 2020.

Salameh, D., Pey, J., Bozzetti, C., El Haddad, I., Detournay, A., Sylvestre, A., Canonaco, F., Armengaud, A., Piga, D., Robin, D., Prevot, A. S. H., Jaffrezo, J.-L., Wortham, H., and Marchand, N.: Sources of $PM_{2.5}$ at an urban-industrial Mediterranean city, Marseille (France): Application of the ME-2 solver to inorganic and organic markers, Atmos. Res., 214, 263–274, https://doi.org/10.1016/j.atmosres.2018.08.005, 2018.

Salameh, T., Sauvage, S., Afif, C., Borbon, A., and Locoge, N.: Source apportionment vs. emission inventories of non-methane hydrocarbons (NMHC) in an urban area of the Middle East: local and global perspectives, Atmos. Chem. Phys., 16, 3595–3607, https://doi.org/10.5194/acp-16-3595-2016, 2016.

Shrivastava, M., Cappa, C., Fan, J., Goldstein, A., Guenther, A., Jimenez, J., Kuang, C., Laskin, A., Martin S., Ng, N., Petaja, T., Pierce, J., Rasch, P., Roldin, P., Senfeld, J., Shiling, J., Smith, J., Thornton, J., Volkamer, R., Wang, J., Worsnop, D., Zaveri, R., Zelenyuk, A., Zhang, Q.: secondary organic aerosol: Implications for global climate forcing. Rev. Geophys., 55, 509–559. https://doi.org/10.1002/2016RG000540, 2017.

Song, Y., Tang, X., Xie, S., Zhang, Y., Wei, Y., Zhang, M., Zeng, L., and Lu, S.: Source apportionment of $PM_{2.5}$ in Beijing in 2004, J. Hazard. Mater., 146, 124–130, https://doi.org/10.1016/j.jhazmat.2006.11.058, 2007.

Tao, J., Zhang, L., Gao, J., Wang, H., Chai, F., and Wang, S.: Aerosol chemical composition and light scattering during a winter season in Beijing, Atmos. Environ., 110, 36–44, https://doi.org/10.1016/j.atmosenv.2015.03.037, 2015.

Wang, Q.; Han, Y.; Ye, J.; Liu, S.; Pongpiachan, S.; Zhang, N.; Han, Y.; Tian, J.; Wu, C.; Long, X.; Zhang, Q.; Zhang, W.; Zhao, Z.; Cao, J.: High Contribution of secondary brown carbon to aerosol light absorption in the southeastern margin of Tibetan Plateau. Geophys. Res. Lett. 46, 4962−4970, https://doi.org/10.1029/2019GL082731, 2019.

Wang, Z., Wang, R., Wang, J., Wang, Y., McPherson Donahue, N., Tang, R., Dong, Z., Li, X., Wang, L., Han, Y., and Cao, J.: The seasonal variation, characteristics and secondary generation of $PM_{2.5}$ in Xi'an, China, especially during pollution events, Environ. Res., 212, 113388, https://doi.org/10.1016/j.envres.2022.113388, 2022.

Xu, H., Cao, J., Chow, J. C., Huang, R.-J., Shen, Z., Chen, L. W. A., Ho, K. F., and Watson, J. G.: Inter-annual variability of wintertime $PM_{2.5}$ chemical composition in Xi'an, China: Evidences of changing source emissions, Sci. Total Environ., 545–546, 546–555, https://doi.org/10.1016/j.scitotenv.2015.12.070, 2016.

Xu, X., Zhang, H., Chen, J., Li, Q., Wang, X., Wang, W., Zhang, Q., Xue, L., Ding, A., and Mellouki, A.: Six sources mainly contributing to the haze episodes and health risk assessment of $PM_{2.5}$ at Beijing suburb in winter 2016, Ecotoxicol. Environ. Saf., 166, 146–156, https://doi.org/10.1016/j.ecoenv.2018.09.069, 2018.

Zhang, Q., Shen, Z., Cao, J., Zhang, R., Zhang, L., Huang, R.-J., Zheng, C., Wang, L., Liu, S., Xu, H., Zheng, C., and Liu, P.: Variations in $PM_{2.5}$, TSP, BC, and trace gases (NO_2, SO_2, and O_3) between haze and non-haze episodes in winter over Xi'an, China, Atmos. Environ., 112, 64–71, https://doi.org/10.1016/j.atmosenv.2015.04.033, 2015.

Zhang, R., Jing, J., Tao, J., Hsu, S.-C., Wang, G., Cao, J., Lee, C. S. L., Zhu, L., Chen, Z., Zhao, Y., and Shen, Z.: Chemical characterization and source apportionment of $PM_{2.5}$ in Beijing: seasonal perspective, Atmos. Chem. Phys., 13, 7053–7074, https://doi.org/10.5194/acp-13-7053-2013, 2013.

Zhang, W., Liu, B., Zhang, Y., Li, Y., Sun, X., Gu, Y., Dai, C., Li, N., Song, C., Dai, Q., Han, Y., and Feng, Y.: A refined source apportionment study of atmospheric $PM_{2.5}$ during winter heating period in Shijiazhuang, China, using a receptor model coupled with a source-oriented model, Atmos. Environ., 222, 117157, https://doi.org/10.1016/j.atmosenv.2019.117157, 2020.

Zhao, P. S., Dong, F., He, D., Zhao, X. J., Zhang, X. L., Zhang, W. Z., Yao, Q., and Liu, H. Y.: Characteristics of concentrations and chemical compositions for $PM_{2.5}$ in the region of Beijing, Tianjin, and Hebei, China, Atmos. Chem. Phys., 13, 4631–4644, https://doi.org/10.5194/acp-13-4631-2013, 2013.